J. Membrane Biol. 140, 197–204 (1994)

The Journal of
Membrane
Biology

Atomic Force Microscopy of Peritoneal Macrophages after Particle Phagocytosis

M. Beckmann, H.-A. Kolb, F. Lang
University of Tübingen, Institute of Physiology I, Gmelinstr. 5, D-72076 Tübingen, Germany

Received: 16 November 1993/Revised: 2 March 1994

Abstract. The atomic force microscope was used to image peritoneal macrophages after phagocytosis of latex beads with 0.45 μm in diameter and of zymosan particles. The rigidity of the phagocytosed material allowed to image the live membrane at forces below 2 nN. Repeated scanning of the membrane unavoidably caused the protrusion of the beads and increased their virtual height. The influence of fixation by glutaraldehyde on the image and the corresponding force *vs.* distance curves were analyzed and compared. Short treatment with Triton X-100 enabled us to identify intracellular components, such as embedded latex beads, cell nucleus and cytoskeletal strands. The data demonstrate that it is possible to image living cells if they are bolstered by stiff material.

Key words: Atomic force microscope (AFM) — Peritoneal macrophages — Particle phagocytosis — Force *vs.* distance curves

Introduction

It is well known that the resolution for the application of the atomic force microscope (AFM) (Binnig, Quate & Gerber, 1986) depends on the stiffness of the material under investigation and therefore reflects the local solid-state properties of the sample. In the case of hard samples, images at atomic resolution can be obtained (Manne et al., 1991; Ohnesorge & Binnig, 1993) which are dependent on the surface topology and probe geometry (Allen et al., 1992; Radmacher et al., 1992). On biological specimens, molecular resolution was obtained on flat organic model membranes (Weisenhorn et al., 1991; Zasadzinski et al., 1991; Bourdieu, Ronsin & Chatenay, 1993) and on isolated and spread membrane areas with embedded or attached proteins (Worcester, Miller & Bryant, 1988; Hoh et al., 1993; Yang et al., 1993). The AFM has also been applied to living or fixed cells (Butt et al., 1990; Henderson, Haydon & Sakaguchi, 1992; Hörber et al., 1992). Recently, the AFM has been used to study membranes of living RBL-2H3-cells (Chang et al., 1993) and of a cultured line of lung carcinoma cells (Kasas, Gotzos & Celio, 1993). At physiological incubation conditions, the resolution decreases with increasing cell height. Also, the reproducibility decreases due to the sample-tip interaction (Butt et al., 1990; Hörber et al., 1992) and the dynamic behavior of living cells (Fritz, Radmacher & Gaub, 1993).

The success of recording the relief of soft plasma membranes under in vivo conditions is limited by the two-dimensional viscoeleastic properties of the membrane as well as the enclosed cytoplasm and the complex surface topography. The elastic properties are mainly determined by the architecture of the cytoskeleton and are reflected in the coefficients of tension, surface shear and bending (Evans & Parsegian, 1983). The dynamic membrane topography is formed by the largely unknown interaction of the cytoskeleton with microfilaments and microtubuli which form the frequently occurring microvilli and membrane protrusions and enfoldings.

In this presentation, we used the property of murine peritoneal macrophages to phagocytose particles to bolster the cytoplasm. The activation of particle phagocytosis by the reagent zymosan extracted from cell walls of *Saccharomyces cerevisiae* yeasts as well as by latex beads is well known and has been studied extensively with immunological (Wright & Silverstein, 1986) and electrophysiological methods (Kolb & Ubl, 1987). We applied the AFM to analyze the size and distribution of phagocytosed material as well as force *vs.* distance curves at different states of fixation. Furthermore, we used phagocytosis as a tool to improve the tip-sam-

Correspondence to: H.-A. Kolb

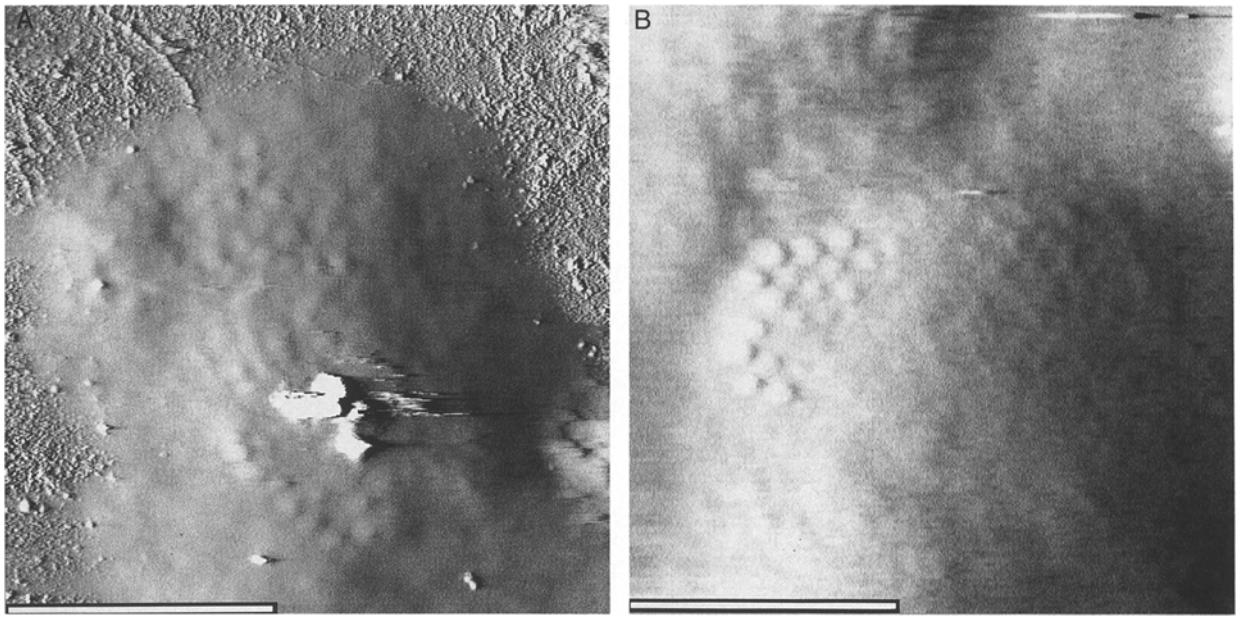

Fig. 1. Live murine peritoneal macrophage after phagocytosis of latex beads of 0.45 μm in diameter. Imaging was carried out in the fluid chamber completely filled with PBS and presented in the shaded mode (*see* Materials and Methods). (*a*) Image after the first scanning. The image of 12 × 12 μm was taken at a scan rate of 23 μm/sec. (*b*) Image after the fifth scanning. Same cell as in *a*. The bar denotes 5 μm, respectively. Maximal scanner area: 25 × 25 μm. Spring constant of the cantilever: 0.064 Nm^{-1}.

ple interaction to image living and fixed membranes of murine peritoneal macrophages in a physiological environment. The degree of membrane wrapping around the latex beads was modulated posteriori by exposure of the cells to Triton X-100. In the latter case, it became possible to image intracellular components and to discriminate membrane covered and uncovered latex beads.

Materials and Methods

Cell Material

Peritoneal macrophages were obtained as previously described (Kolb & Ubl, 1987). Through a small hole in the abdominal wall of a NMRI mouse about 3 ml of HEPES-buffered saline (*see below*) was injected. The abdomen was agitated manually and the solution withdrawn. Cells were washed twice at 300 × *g* and resuspended in culture medium (Dulbecco's modified Eagle medium (DMEM) plus 10% fetal calf serum). The cells were seeded in petri dishes on small pieces obtained from the bottom of those dishes and maintained at 37°C in 95% air and 5% CO_2.

Electrolyte Solutions and Fixation Procedures

The macrophages become spontaneously adherent. After an incubation period of about 30 min the culture medium was replaced. In one series of experiments, the cells were exposed to latex beads of diameter 0.453 ± 0.009 μm (Serva). The corresponding stock solution was diluted 1:1,000 in culture medium. In the case of zymosan A (Sigma), the particles were added at 50 μg/ml to a pure electrolyte (in mM): 140 NaCl, 5.6 KCl, 1.2 $MgCl_2$, 2.6 $CaCl_2$, 0.5 glucose and 10 HEPES, at pH 7.4. The particle suspensions were finally dispersed by sonification for 1 min.

The macrophages were exposed to particle-containing media for a further 60 min at 37°C. Thereafter, the particle suspensions were replaced and the cells were washed under slight pressure to get rid of nonadherent cells. Either zymosan-free electrolyte solution (*see above*) was used or the culture medium was rinsed with a HEPES-buffered saline (HBS) (in mM): 134 NaCl, 4 KCl, 1 $MgCl_2$, 1 $CaCl_2$, 18 glucose, 20 HEPES or a phosphate-buffered saline (PBS) (in mM): 136.9 NaCl, 2.7 KCl, 0.7 $CaCl_2$, 0.4 $MgSO_2$, 0.5 glucose, 1.5 KH_2PO_4, 8.3 Na_2PO_4, 8.3 Na_2PO_4 adjusted to pH 7.4, respectively.

For fixation 1% glutaraldehyde (Serva) was added to the buffer. The cells were kept for 15 min in the presence of the fixans at room temperature and washed with pure electrolyte solutions. After glutaraldehyde treatment and before air-drying, the cells were thoroughly rinsed with distilled water. Prior to fixation, Triton X-100 (Serva) was applied at 37°C for 5 min at 0.1% in HBS.

AFM Imaging

A commercial TMX 2010 (Topometrix) was used. The V-shaped cantilevers had a spring constant of 0.032 Nm^{-1}. For living, unfixed macrophages, those with 0.064 Nm^{-1} or 0.032 Nm^{-1} were applied as indicated. The tip geometry was pyramidal with a base and height of 4 μm, respectively. For determination of force *vs.* distance curves we used an xyz translator (scanner) with a maximal xy scanning area of 7 × 7 μm. Imaging was performed with scanners of 7 × 7 μm, 25 × 25 μm or 75 × 75 μm area and carried out at room temperature. The plastic coverslips were mounted on a metal disc and in a fluid chamber. For imaging under electrolyte solution, the fluid chamber was filled completely. The solutions were filtered through a 0.2 μm millipore filter. The force was monitored prior to imaging and set below 2 nN. The images were taken in the constant force mode which is synonymous with height mode. The commercial software was

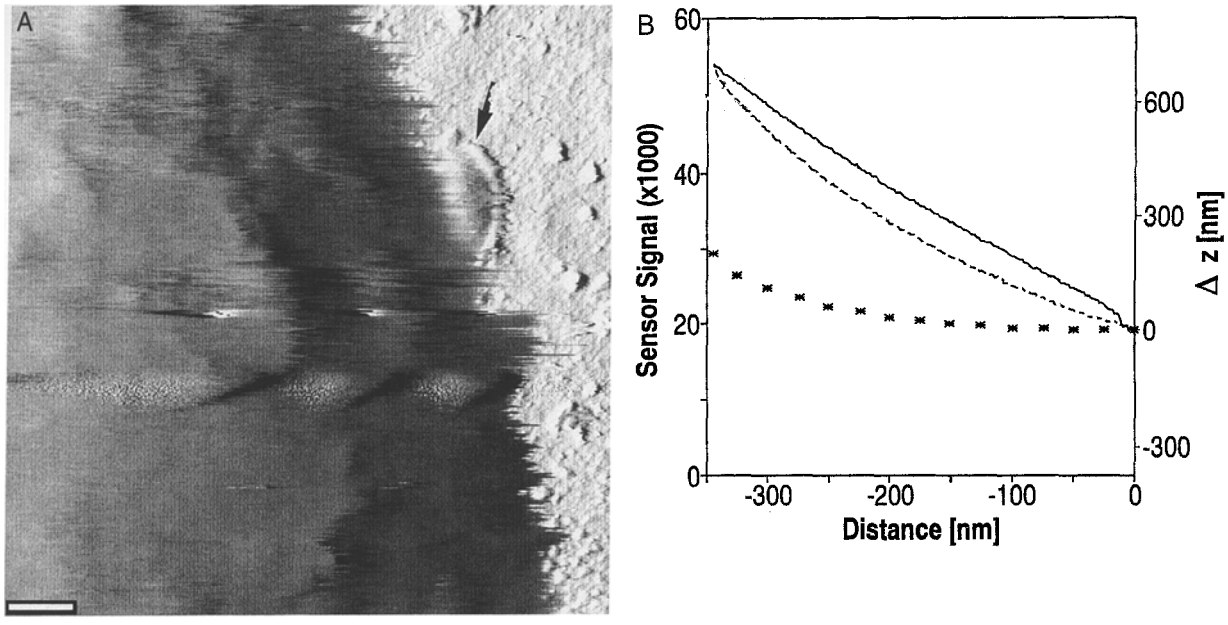

Fig. 2. Live murine peritoneal macrophage after phagocytosis of latex beads (*see* Fig. 1). Imaging and force *vs.* distance curve were carried out in the fluid chamber with PBS at room temperature. (*a*) Image after the first scanning. The arrow denotes part of the adherent membrane close to the plastic coverslip. Image size: 4.9 × 4.9 μm, scan rate 10 μm/sec, bar 500 nm. (*b*) Force *vs.* distance curve at a randomly selected elevated membrane location. The units of the y-axis (left scale) are as read from the AFM with an installed scanner of 7 × 7 μm. The maximal contact force was set to 20 nN which corresponds to the maximal value of the drawn curves, while the minimal value corresponds to 0 nN. The distance of the x-axis is given by the movement of the z-transducer after contact. The unbroken line shows the motion of the sample towards the tip, the dashed line from the tip. The time for a complete circle was less than 1 sec. Spring constant of the cantilever: 0.032 Nm^{-1}. The curve (*) was drawn by use of the relation (Sneddon, 1965; Tao et al., 1992):

$$\Delta z = z + B(1 - \sqrt{(1 + 2\,z/B)})$$

Δz is the cantilever deflection which was derived from the applied force divided by the cantilever spring constant (*see* vertical scaling on the right hand of the figure). z is the distance after contact which corresponds to the negative values on the x-axis. In the constant B, the parameters of the shear rigidity, the Poisson constant and the parameters of geometry of the tip are lumped together. From a least-squares fit, $B = 732$ nm was obtained.

used for leveling and shading with simulated light from the left. By the process of shading, a more plastic image is derived. The corresponding gray scale is not related to the height scale, but to the angle between the surface orientation and the light direction. The image of Fig. 6*b* is unshaded and the corresponding height scale is presented.

Results and Discussion

Prior to imaging, the macrophages were allowed to phagocytose particles of different origin. Figure 1*a* shows a low-magnification image of a living murine peritoneal macrophage with phagocytosed latex beads with a diameter of 0.45 μm in PBS. The surface appeared smooth, but often the top of the cell was too elevated and scan-induced distortions became visible (*see* Fig. 1*a*). Such a quasi-unperturbated image could be obtained for macrophages which were sufficiently rigid after phagocytosis of numerous beads. Chang et al. (1993) hardened the membrane surface of RBL-2H3-cells by crosslinking membrane receptors. In accordance with their observations, we find that the AFM can yield an undistorted image of the plasma membrane of living cells if the support, the cytoskeleton and the cytoplasm are rigid enough. But even in this advantageous case, repeated scanning enhances the relief structure and seems to indent the membrane between the latex beads (Fig. 1*b*). In general, the image of the soft plasma membrane appeared in electrolyte solution as shown in Fig. 2*a*. Clear images of flattened membrane areas close to the surface of the substrate are visible (*see arrow*), as well as elevated membrane areas obviously deformed by the imaging tip, even with forces of about 0.5 nN (*compare* Häberle, Hörber & Binnig, 1991; Yang et al., 1993) and low-scan rate (*see* figure legend). The latter appears as smearing or lateral deformation which is most probably caused by the cantilever indenting or even penetrating the intact membrane (*see also* Henderson et al., 1992) and the scanning movement from left to right. Similar observations were made for untreated macrophages. The figure indicates that already forces of this low magnitude might cause scan-induced

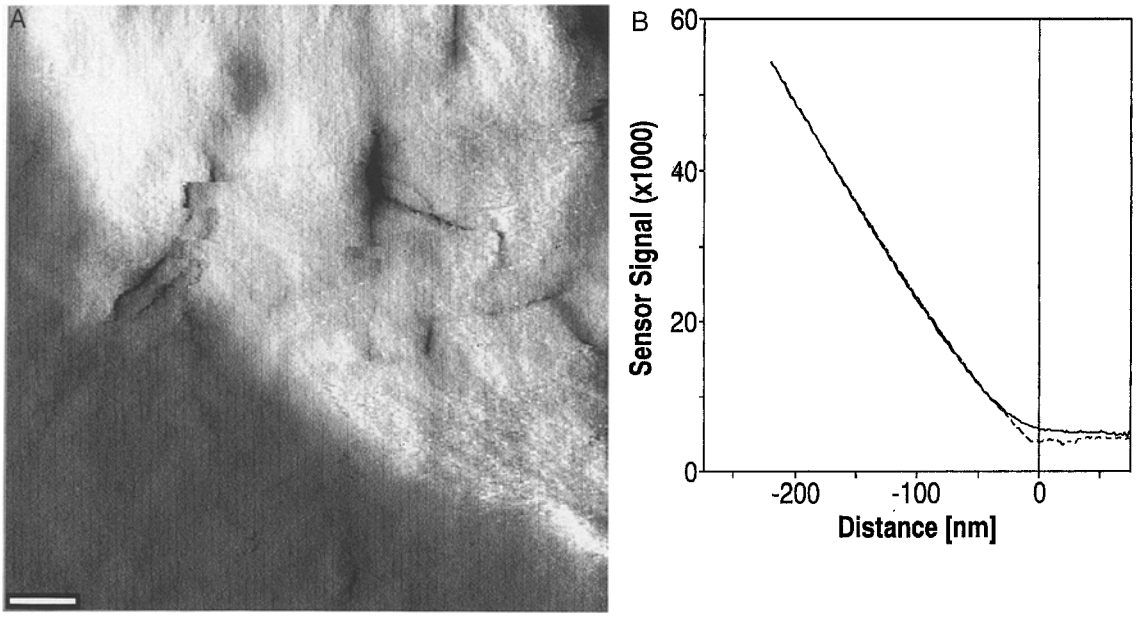

Fig. 3. Fixed (1% glutaraldehyde) murine peritoneal macrophage after phagocytosis of latex beads. Imaging and the force *vs.* distance curve were carried out in the fluid chamber with HBS at room temperature. (*a*) Image after the first scanning. Bar: 500 nm. (*b*) Force *vs.* distance curve at a randomly selected membrane location. The unbroken line shows the motion of the sample towards the tip, the dashed line from the tip. The units of the y-axis are as given by the AFM with an installed scanner of 7 × 7 μm. The maximal force was set to 20 nN, while the minimal value corresponds to 0 nN. The time for a complete circle was less than 1 sec. Spring constant of the cantilever: 0.032 Nm^{-1}.

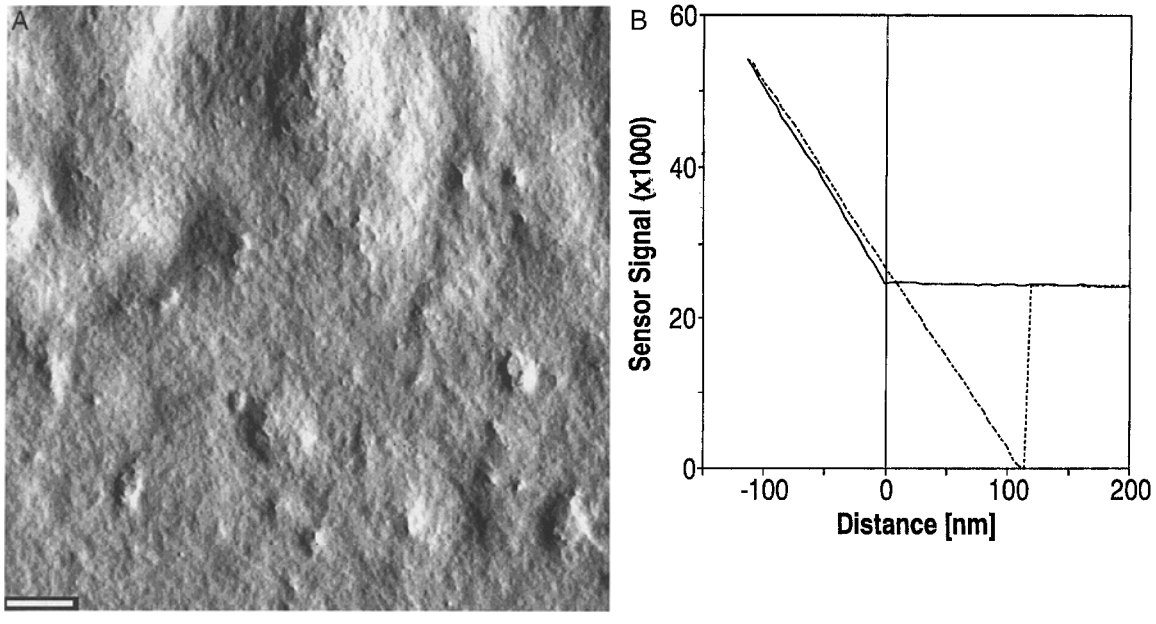

Fig. 4. Fixed (1% glutaraldehyde) and air-dried murine peritoneal macrophage after phagocytosis of latex beads. (*a*) Image after the first scanning. Bar: 500 nm. (*b*) Force *vs.* distance curve at a randomly selected membrane location. The unbroken line shows the motion of the sample towards the tip, the dashed line from the tip. Positive distances correspond to attractive forces. The units of the y-axis are as given by the AFM with an installed scanner of 7 × 7 μm. The maximal force was set to 20 nN, while the value at positive distance from the membrane corresponds to 0 nN. The time for a complete circle was less than 1 sec. Spring constant of the cantilever: 0.032 Nm^{-1}.

deformation on living cells which were observed less often for fixed and/or dried macrophages (*see below*). The image could not be improved by reducing the scan-rate to a tenth of the total image size per second. As Persson (1987) pointed out, even a local force of the substrate-tip interaction in the order of 0.01 nN causes deformations when studying soft biological materials.

The local elasticity of the sample can be estimated

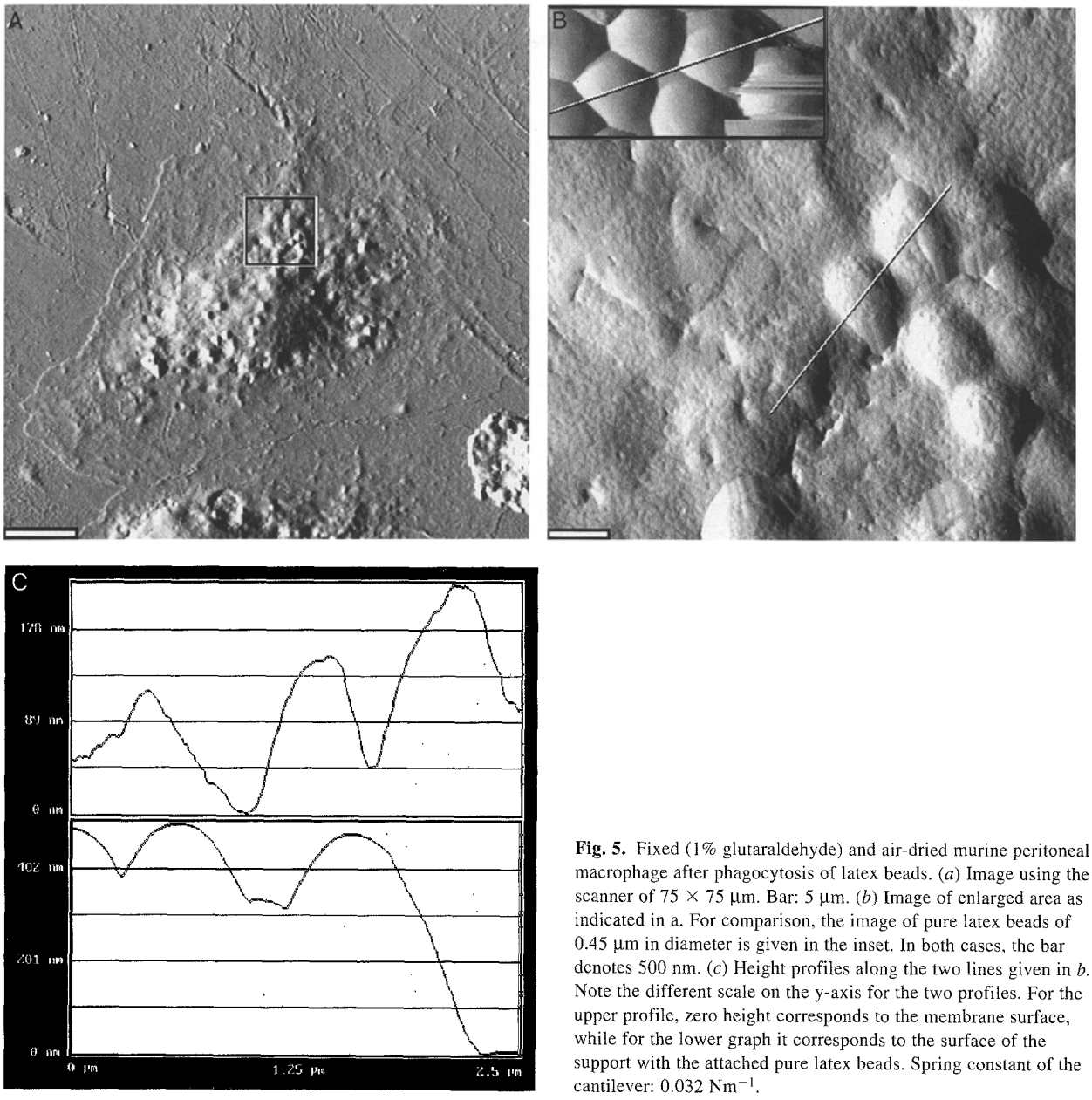

Fig. 5. Fixed (1% glutaraldehyde) and air-dried murine peritoneal macrophage after phagocytosis of latex beads. (*a*) Image using the scanner of 75 × 75 µm. Bar: 5 µm. (*b*) Image of enlarged area as indicated in a. For comparison, the image of pure latex beads of 0.45 µm in diameter is given in the inset. In both cases, the bar denotes 500 nm. (*c*) Height profiles along the two lines given in *b*. Note the different scale on the y-axis for the two profiles. For the upper profile, zero height corresponds to the membrane surface, while for the lower graph it corresponds to the surface of the support with the attached pure latex beads. Spring constant of the cantilever: 0.032 Nm^{-1}.

from modulation of the vertical sample position yielding to a modulation of the force between tip and sample. The corresponding force *vs.* distance curve (*see* Fig. 2*b*) reveals a hysteresis of repulsive forces depending on the polarity of the distance change. Attractive forces are minimized by the electrolyte in the fluid chamber and were not observed (*compare* Lyubchenko et al., 1993). This means that the vertical interaction between tip and sample is dominated by an elastic indentation rather than by an adhesion between tip and sample. For determination of the data given in Fig. 2*b*, the maximal applied force was set to 20 nN which would correspond to a cantilever deflection of 625 nm at a spring constant of 0.032 Nm^{-1}. From Fig. 2*b*, we derived a slope of 0.05 Nm^{-1} at −100 nm. The slope can be considered as the effective stiffness of the tip-sample system which is a factor of 10 smaller than measured for Cd-arachidate monolayers (Radmacher et al., 1992). The derived value of the slope is in the order of the spring constant of the used cantilever. Therefore, occasionally the image of the cantilever was obtained and the macrophage could be considered as cantilever (*data not shown*). For a quantitative description of the force *vs.* distance curve, we used the approach of Tao, Lindsay and Lees (1992). The theoretical description is given in the legend of Fig. 2*b*. The corresponding curve is indicated by stars. The figure shows that this description of microelastic properties of biological material cannot be applied to describe the course of the measured tip-sample interaction.

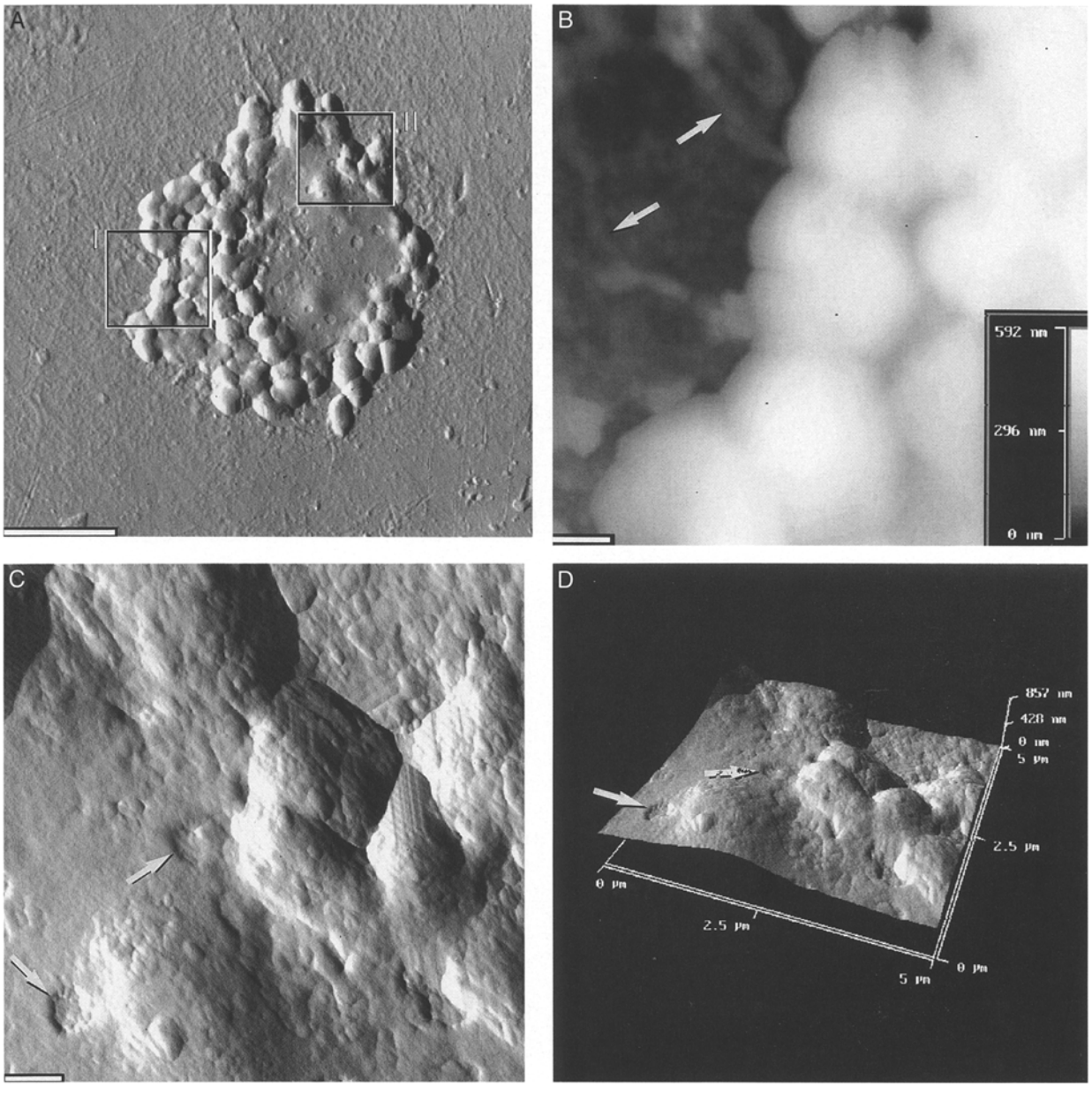

Fig. 6. Triton-treated (0.1% Triton X-100 for 5 min) and air-dried murine peritoneal macrophage after phagocytosis of latex beads. (*a*) Image of a macrophage. Bar: 5 μm. Note that the transition membrane to coverslip is not visible. The latex beads appear to be partially covered by the membrane. (*b*) Unshaded image of the area denoted as | in *a*. Arrows denote examples of cytoskeletal strands. Bar: 500 nm. (*c* and *d*) Two- and three-dimensional image of a part of the membrane and the underlying latex beads corresponding to area || of *a*. Arrows denote holes in the plasma membrane caused by Triton. Bar: 500 nm. Maximal scanner area: 75 × 75 μm. Spring constant of the cantilever: 0.032 Nm^{-1}.

The elastic deformation of the sample can be most simply characterized by the work required to change area, surface shear, and binding of the membrane. For red cells, it has been measured that the elastic coefficients for increase of membrane surface area (tension) are up to six orders of magnitude greater than the elastic coefficients for surface extension and bending (Evans & Parsegian, 1983). A maximal tension that produced lysis of red cells was observed to be 0.03–0.04 Nm^{-1} (Kwok & Evans, 1981). Comparison with the above value suggests that the local vertical deformation could yield membrane rupture and that the force *vs.* distance curve is determined by the surface tension.

For comparison, a force *vs.* distance curve of a glutaraldehyde-fixed plasma membrane in HBS is presented in Fig. 3*b*. The force *vs.* distance curve for the down and up movement of the sample shows an about straight line with a slope of 0.11 Nm^{-1} at −100 nm

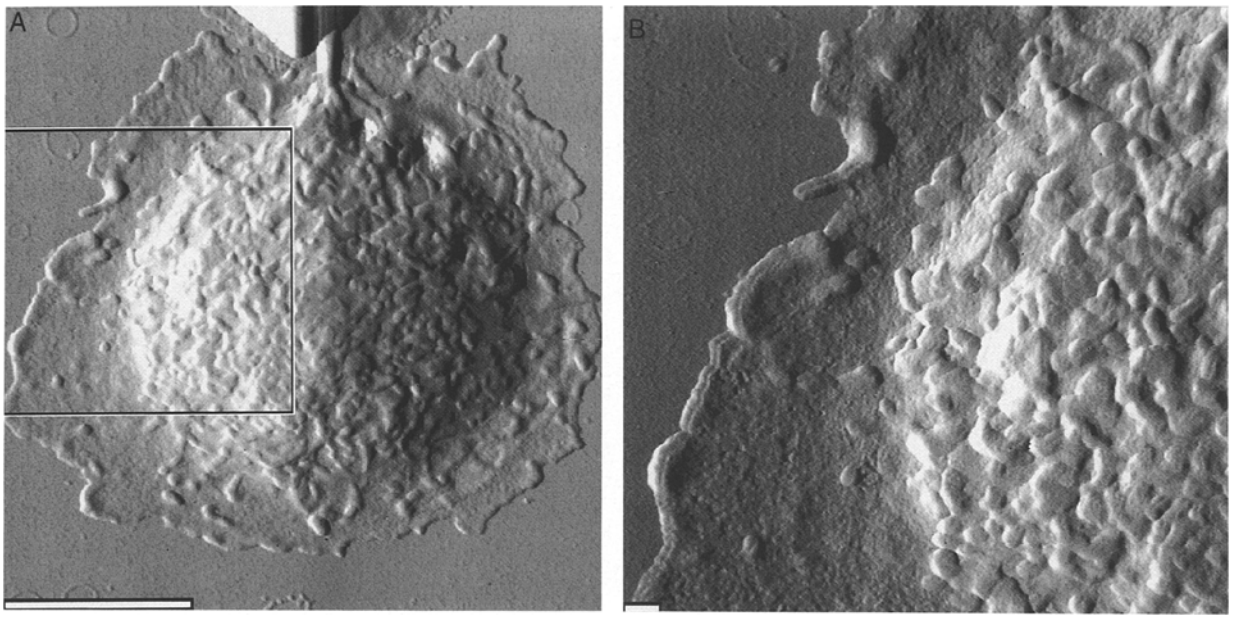

Fig. 7. Fixed (1% glutaraldehyde for 15 min) murine peritoneal macrophage after phagocytosis of zymosan particles. Imaging was carried out in the fluid chamber with HBS at room temperature. (*a*) Image size is 17 × 17 μm. Bar: 5 μm. (*b*) Image of the area indicated in *a*. The bar denotes 500 nm. Maximal scanner area: 25 × 25 μm. Spring constant of the cantilever: 0.032 Nm^{-1}.

which is about twice as large as observed with live macrophages. At distances larger than −30 nm, variations can be seen which might be responsible for distortions shown in the corresponding image (Fig. 3*a*).

In the force *vs.* distance curve obtained under air-dried conditions, the transition from the nontouching to the touching condition of the tip becomes clearly visible during the down movement (Fig. 4*b*). A slope of 0.18 Nm^{-1} is obtained. It means that air-drying only causes a further increase of the slope by less than a factor of two. At larger forces, air-drying has no further significant influence on the slope of the force *vs.* distance curve (*compare* Figs. 3*b* and 4*b*). Longer fixation with glutaraldehyde of increasing concentration and/or drying did not result in steeper slopes (*not shown*). Furthermore, an attractive pull-out force (Israelachvili, 1985) of about 16 nN can be read from the dashed curve of Fig. 4*b* which is in the range obtained by Lyubchenko et al. (1993).

The increasing values for the slope of the force *vs.* distance curves as a function of cell fixation are reflected in the apparent membrane property presented in Figs. 2*a*, 3*a* and 4*a*. A comparison indicates that the contrast of the image which appears to be virtually related to the stiffness of the membrane surface increases with increasing degree of fixation.

The image of a fixed and air-dried macrophage is presented in Fig. 5. Comparison with the image obtained under in vivo conditions (Fig. 1) shows that the fixation procedure changes significantly the topology of the cell surface. The smooth surface is transformed to a surface composed of enfoldings and bulgings. The latex beads emerge out of the membrane which allows their closer inspection. On magnified images (Fig. 5*b*), the latex beads can be identified by the shape of the wrapping membrane which is confirmed by the corresponding height profile (Fig. 5*c*). A lateral resolution in the order of about 50 nm was obtained. For comparison, the image and height profile of pure latex beads are shown in Fig. 5*b* and *c*. The height of the pure latex beads closely agrees with the diameter of about 450 nm for the beads. It is known that the height of the object is affected only by the compressibility of the object, while the width is additionally affected by the sharpness or geometry of the tip (Allen et al., 1992). Due to the specific pyramidal geometry of the tip (*see* Materials and Methods), the derived spacing for the latex beads in Fig. 5*c* gives only an upper estimate.

Treatment of macrophages with Triton X-100 allows the identification of cytoskeletal structures and the unwrapping of the phagocytosed latex beads. Figure 6 shows the image after a mild treatment with 0.1% Triton X-100 for 5 min. In Fig. 6*a*, the transition between plasma membrane and substrate is not visible. But in a magnified and unshaded image (Fig. 6*b*) fibrous structures are apparent along the rim (*see arrow*) with a height of 15–40 nm and a width of about 150 nm. Similar structures have been observed with AFM (Henderson et al., 1992; Chang et al., 1993) which have been recognized as bundled actin filaments. These structures are hardly visible in the shaded mode (*see* Fig. 6*a*). An enlarged image of phagocytosed beads shows

areas of membrane covered and uncovered surfaces (Fig. 6*c* and *d*). In the latter case, cytoskeletal elements could not be identified around phagocytosed latex beads. This observation supports the hypothesis of Wright and Silverstein (1986) that cytoskeletal elements are not involved in the ingestion process of small (<1 μm) latex beads.

Figure 7 shows a fixed (glutaraldehyde) macrophage after phagocytosis of zymosan particles. The image was taken in HBS. The shape of the elongated particles can be recognized from Fig. 7*b*. As in the case of phagocytosed latex balls (Fig. 1), the membrane appears as a characteristic relief-like structure formed by the zymosan particles.

The data indicate that the main problem for AFM of biological material is the softness of the samples which is reflected in the shape and slope of the force *vs.* distance curve. In our case, the smallest possible imaging force of about 0.5 nN is not sufficient for an undistorted scan of live cell membranes at elevated parts of untreated macrophages. Yet, after particle phagocytosis, macrophages are sufficiently rigid for imaging. With further minimizing of the imaging force and experimentation with surface treatment, much can be done to elucidate the details of a single phagocytotic event.

The authors wish to thank Dr. H. Oberleithner for his generous support, helpful discussions and the suggestion of Triton treatment. The authors gratefully acknowledge Dr. I. Jahns for establishing the AFM technique at the Institute of Physiology. The work was supported by the Deutsche Forschungsgemeinschaft Projekt No. La 315/4-1.

References

Allen, M.J., Hud, N.V., Balooch, M., Tench, R.J., Siekhaus, W.J., Balhorn, R. 1992. Tip-radius-induced artifacts in AFM images of protamine-complexed DNA fibers. *Ultramicroscopy* **42–44:**1095–1100

Binnig, G., Quate, C.F., Gerber, C. 1986. Atomic force microscope. *Phys. Rev. Lett.* **56:**930–933

Bourdieu, L., Ronsin, O., Chatenay, D. 1993. Molecular positional order in Langmuir-Blodgett films by atomic force microscopy. *Science* **259:**798–801

Butt, H.-J., Wolff, E.K., Gould, S.A.C., Northern, B.D., Peterson, C.M., Hansma, P.K. 1990. Imaging cells with the atomic force microscope. *J. Struct. Biol.* **105:**54–61

Chang, L., Kious, T., Yorgancioglu, M., Keller, D., Pfeiffer, J. 1993. Cytoskeleton of living, unstained cells imaged by scanning force microscopy. *Biophys. J.* **64:**1282–1286

Evans, E., Parsegian, V.A. 1983. Energetics of membrane deformation and adhesion in cell and vesicle aggregation. *Ann. NY Acad. Sci.* **416:**13–33

Fritz, M., Radmacher, M., Gaub, H.E. 1993. *In vitro* activation of human platelets triggered and probed by atomic force microscopy. *Exp. Cell Res.* **205:**187–190

Häberle, W., Hörber, J.K.H., Binnig, G. 1991. Force microscopy on living cells. *J. Vac. Sci. Technol.* [*B*] **9:**1210–1213

Henderson, E., Haydon, P.G., Sakaguchi, D.S. 1992. Actin filament dynamics in living glial cells imaged by atomic force microscopy. *Science* **257:**1944–1946

Hoh, J.H., Sosinsky, G.E., Revel, J.-P., Hansma, P.K. 1993. Structure of the extracellular surface of the gap junction by atomic force microscopy. *Biophys. J.* **65:**149–163

Hörber, J.K., Häberle, W., Ohnesorge, F., Binnig, G., Liebich, H.G., Czerny, C.P., Mahnel, H., Mayr, A. 1992. Investigation of living cells in the nanometer regime with the scanning force microscope. *Scanning Microsc.* **6:**919–929

Israelachvili, J.N. 1985. Chapter 14: Adhesion. *In:* Intermolecular and Surface Forces. pp. 213–226. Academic, London

Kasas, S., Gotzos, V., Celio, M.R. 1993. Observation of living cells using the atomic force microscope. *Biophys. J.* **64:**539–544

Kolb, H.-A., Ubl, J. 1987. Activation of anion channels by zymosan particles in membranes of peritoneal macrophages. *Biochim. Biophys. Acta* **899:**239–246

Kwok, R., Evans, E. 1981. Thermoelasticity of large lecithin bilayer vesicles. *Biophys. J.* **35:**637–652

Lyubchenko, Y.L., Oden, P.I., Ilampner, D., Lindsay, S.M., Dunker, K.A. 1993. Atomic force microscopy of DNA and bacteriophage in air, water and propanol: The role of adhesion forces. *Nucleic Acids Res.* **21:**1117–1123

Manne, S., Hansma, P.K., Massie, J., Elings, V.B., Gewirth, A.A. 1991. Atomic-resolution electrochemistry with the atomic force microscope: Copper deposition on gold. *Science* **251:**183–186

Ohnesorge, F., Binnig, G. 1993. True atomic resolution by atomic force microscopy through repulsive and attractive forces. *Science* **260:**1451–1456

Persson, B.N.J. 1987. The atomic force microscope: Can it be used to study biological molecules? *Chem. Phys. Lett.* **141:**366–368

Radmacher, M., Tillmann, R.W., Fritz, M., Gaub, H.E. 1992. From molecules to cells: Imaging soft samples with the atomic force microscope. *Science* **257:**1900–1905

Sneddon, I.N. 1965. The relation between load and penetration in the axisymmetric Boussinesq problem for a punch of arbitrary profile. *Int. J. Eng. Sci.* **3:**47–56

Tao, N.J., Lindsay, S.M., Lees, S. 1992. Measuring the microelastic properties of biological material. *Biophys. J.* **63:**1165–1169

Weisenhorn, A.L., Egger, M., Ohnesorge, F., Gould, S.A.C., Heyn, S.-P., Hansma, H.G., Sinsheimer, R.L., Gaub, H.E., Hansma, P.K. 1991. Molecular-resolution images of Langmuir-Blodgett films and DNA by atomic force microscopy. *Langmuir* **7:**8–12

Worcester, D.L., Miller, R.G., Bryant, P.J. 1988. Atomic force microscopy of purple membranes. *J. Microsc.* **152:**817–821

Wright, S.D., Silverstein, S.C. 1986. Overview: The function of receptors in phagocytosis. *In:* Handbook of Experimental Immunology. Volume 2: Cellular Immunology. D.M. Weir, L.A. Herzenberg, C. Blackwell and L.A. Herzenberg, editors, pp. 41.1–41.14. Blackwell Scientific Publications, Oxford, UK

Yang, J., Tamm, L.K., Tillack, T.W., Shao, Z. 1993. New approach for atomic force microscopy of membrane proteins. The imaging of cholera toxin. *J. Mol. Biol.* **229:**286–290

Zasadzinski, J.A.N., Helm, C.A., Longo, M.L., Weisenhorn, A.L., Gould, S.A.C., Hansma, P.K. 1991. Atomic force microscopy of hydrated phosphatidylethanolamine bilayers. *Biophys. J.* **59:**755–759